

ESTIMATION OF KINETIC PARAMETERS FROM CONVERSION CURVES, DETERMINED AT CONSTANT HEATING RATE

R. ALTORFER

Mettler Instrumente AG, CH-8606 Greifensee (Switzerland)

(Received 22 July 1977)

ABSTRACT

A new method is described to evaluate kinetic parameters from conversion curves by using non-linear regression analysis. The method is based on the model of pseudohomogeneous kinetics and assumes an irreversible reaction.

Experimental data in the form of a conversion curve, determined at constant heating rate, have to be available.

An implementation of this method was tested with simulated curves and applied to the decomposition reaction of CaCO_3 , measured by TG-analysis.

It is shown that, in order to suppress the reverse reaction, a flow of inert gas at low pressure has to be maintained. This in turn demands the use of the new evaluation method in order to cope with the stronger measuring fluctuations existing under these conditions.

1. INTRODUCTION

Many heterogeneous decomposition reactions of solids are described by the model of pseudohomogeneous kinetics which assumes the following time-dependence of the conversion degree $\alpha(t)$

$$\frac{d\alpha}{dt} = k(T) (1 - \alpha)^v \quad (1)$$

where, according to Arrhenius

$$k(T) = F e^{-E/RT} \quad (2)$$

T = absolute temperature; F = frequency factor; E = activation energy; v = reaction order.

For the moment, however, only phenomenological significance may be attributed to the kinetic parameters F , E , v .

They are preferably determined by methods requiring the measurement of only one decomposition curve, thus demanding measurement at dynamic temperature control.

The advantage of such methods has become somewhat questionable owing to the fact that the results show considerable deviations¹. This becomes comprehensible when one considers the conditions that have to be fulfilled to enable an ideal course of reaction according to eqn (1).

The first pre-condition is a well-defined and homogeneous sample temperature. Secondly, no reverse reaction is allowed to take place, which implies negligible partial pressure of the decomposition gas. Since, during the whole reaction, there is a continuous flow of gas and heat within the sample, these ideal requirements may never entirely be fulfilled.

Considering the varying apparatus and measuring conditions generally used, differences in results are to be expected. In order to meet the ideal conditions as far as possible, the use of small samples and low heating rates have been recommended².

Of interest seems the fact that by evaluation of one and the same conversion curve $\alpha(t)$ with different methods, considerable differences between the resulting kinetic parameter sets may arise^{2, 3}. Therefore, a closer inspection of these methods is appropriate. Most of them are based on measurements at constant heating rate, i.e., sample temperature increasing linearly in time, this always being assumed below. Therefore

$$T = T_A + \phi t$$

$$\phi = \frac{dT}{dt} = \text{const.} \quad (3)$$

T_A = starting temperature; ϕ = heating rate.

The performing of the variable transformation $t \rightarrow T$ in (1) yields together with (2)

$$\frac{dz}{dT} = \frac{F}{\phi} e^{-E/RT} (1 - \alpha)^{\nu} \quad (4)$$

Nearly all methods operate with a fixed reaction order which either has to be known in advance or must be determined by trial and error. Frequently, only the values $\nu = \frac{1}{2}, \frac{2}{3}$ are taken into consideration, corresponding to the theoretically found values for reactions taking place at interfaces, moving at constant speed in grains or compacted samples of cylindrical or spherical shape.

The method of Freeman-Carroll (FC)^{4, 5} which proceeds from the logarithmic form of eqn (4) and uses numerical differentiation, seems to be the only one within the frequently employed methods which also determines the order of reaction directly. Caused by numerical differentiation procedure, this method is subject to a high sensitivity to experimental fluctuations, which are always present in the conversion curves⁴. Moreover, the linear regression analysis applied to the special form of the original reaction equation involves different weighting of the distinct measuring points corresponding to their varying values of conversion α .

For a better determination of kinetic parameters, a new method is presented

first. It has been developed in order to comply with the following requirements:
 direct and simultaneous determination of the three kinetic parameters F , E , ν
 belonging to the conversion curves;

integral method, i.e., without numerical differentiation;

optimization criterion: least sum S of squares of the residues $\Delta\alpha_i$ (differences between optimal model curve and experimentally determined conversion data):

$$S \equiv \sum_i (\Delta\alpha_i)^2 \rightarrow \min \quad (5)$$

Sum S may basically be considered as a non-linear function of the kinetic parameters, the minimum of their sum has to be determined.

Many of the methods used for optimization of non-linear functions work iteratively. The frequently applied hill-climbing or direct-search methods^{6, 7} need in general a large number of iteration steps; this in contrast to non-linear regression (NLR) which is known as rapidly convergent, particularly towards the end of the evaluation⁸, provided convergence exists at all.

It was therefore decided to develop the NLR-method, as it is considered most promising respecting the evaluation of kinetic parameters. The main problem remaining then consisted in assuring convergence for all practical cases to be attempted. On account of the introduction of a modified set of kinetic parameters, the NLR-method proved successful.

Matters were complicated by the fact that the regression had to be applied to a problem which is described by a differential equation not solvable in analytical form.

Finally, to obtain information on the practical performance, the method was applied to the decomposition reaction of lime



a problem that had previously been investigated many times. Of special interest was the influence of the measuring conditions on the resulting kinetic parameters.

2. THEORY

2.1. General

The above-mentioned modification of the parameter-set consisted in replacing the frequency factor F by a new parameter ψ , called "frequency variable", which has been defined by

$$F = F_A e^\psi \leftrightarrow \psi = \ln \left(\frac{F}{F_A} \right) \quad (6)$$

F_A = assessed initial value of frequency factor.

This modification caused a decisive improvement of the convergence behaviour by enabling much larger iteration steps without risk of divergence.

The reaction equation may now be given in modified form

$$\frac{d\alpha}{dT} = \frac{F_A}{\Phi} e^{\psi - E/RT} (1 - \alpha)^\nu \quad (7)$$

With given values for F_A , ϕ every solution $\alpha(T)$ of the differential eqn (7) may be characterized by the corresponding parameter triple (ψ, E, ν) . The evaluated triple values evolving from a measured curve are then identical with the parameters of that special solution of eqn (7) best adapted to the measurements with respect to the optimization criterion (5).

The associated frequency factor F is then calculated from F_A and ψ by means of eqn (6).

According to the general proceeding in non-linear regression⁹, the kinetic parameters are united in a vector

$$\mathbf{x} = \begin{bmatrix} \psi \\ E \\ \nu \end{bmatrix} \quad (8)$$

The function $\alpha(x, T)$ may be considered as a sequence of data points, given at discrete temperature values T_i (i.e., with constant intervals) leading to a representation as an m -dimensional vector $\alpha(x)$, with the i th component

$$[\alpha(x)]_i \equiv \alpha(x, T_i) \quad (9)$$

After expanding in a Taylor series up to only linear terms (linear approximation) we have

$$\alpha(x) = \alpha(x^0) + \text{grad } \alpha|_{x=x^0} \xi = \alpha(x^0) + C\xi \quad (10)$$

with

$$\xi = x - x^0 = \Delta x \quad (11)$$

and the gradient matrix

$$C \equiv \text{grad } \alpha|_{x=x^0} = C(x^0) \quad (12)$$

whereby

$$C_{ij} = \left. \frac{\partial \alpha_i}{\partial x_j} \right|_{x=x^0} = \left. \frac{\partial \alpha(x, T)}{\partial x_j} \right|_{\substack{x=x^0 \\ T=T_i}} \quad (13)$$

In order to calculate the gradient matrix, three non-linear differential equations have to be solved, as will be shown in section 2.2.

Let l be the conversion vector, determined from measurements; the following residue vectors are then defined

$$\left. \begin{aligned} r &\equiv \alpha(x) - l \\ r^0 &\equiv \alpha(x^0) - l \end{aligned} \right\} \quad (14)$$

so that eqn (5) demanding optimum conformity of vectors α and l may be expressed as

$$(r, r) = \min \rightarrow \text{grad } (r, r) = 0 \quad (15)$$

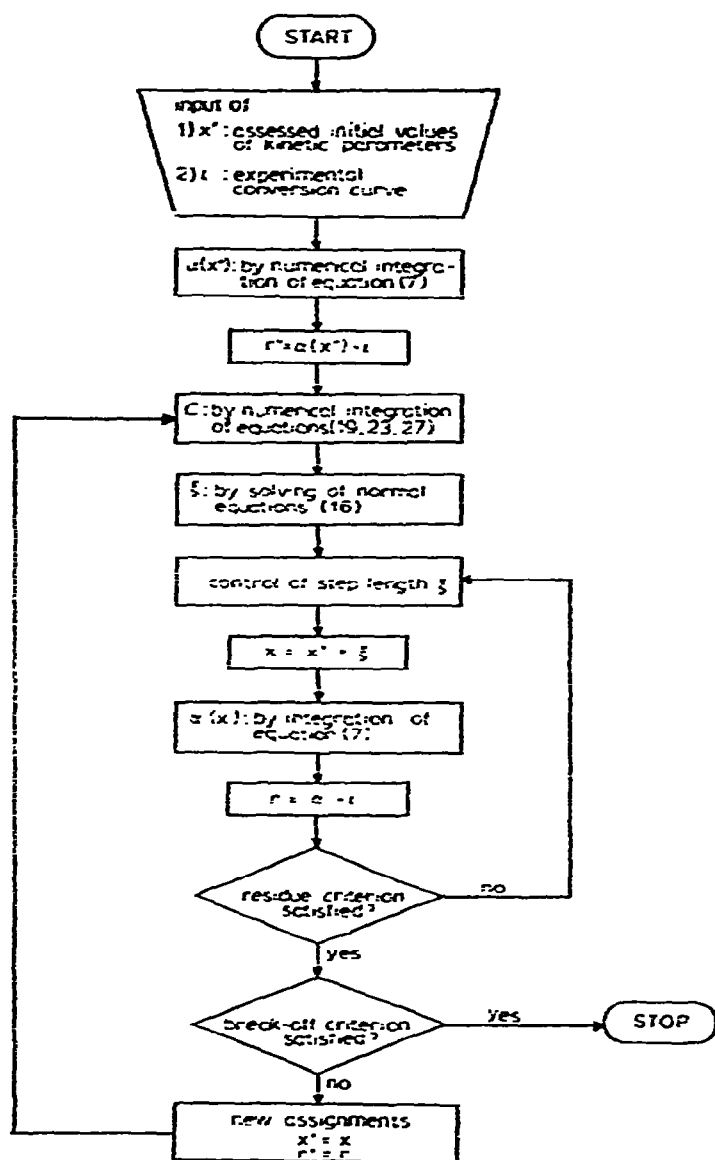


Fig. 1. Flow-chart diagram of iteration procedure (principle).

Inserting (14) and (10), one obtains the so-called Gaussian normal equations

$$C^T C \xi + C^T r_0 = 0 \quad (16)$$

This is a system of three linear equations with the three components of vector ξ as unknowns, representing the parameter corrections evolving from the actual iteration step.

The kinetic parameters belonging to a certain conversion vector l may then be determined iteratively by performing the whole procedure repeatedly, as shown in Fig. 1.

With appropriately chosen initial values and limiting quantities (see section 2.3), the procedure converges: the absolute value of the correction vector decreases in the course of the iteration procedure to infinitesimal values; consequently the linear approximation is increasingly valid.

2.2. Calculation of gradient matrix

C_{i1} . By definition

$$C_{i1} \equiv \left. \frac{\partial x}{\partial \psi} \right|_{\substack{x=x^0 \\ T=T_1}} \quad (17)$$

Performing partial differentiation with respect to ψ in eqn (7), one obtains for $v \neq -1$

$$\frac{\partial^2 x}{\partial \psi \partial T} = \frac{F_0}{\Phi} e^{\psi - E/RT} (1-x)^v \left[1 - \frac{v}{1-x} \frac{\partial x}{\partial \psi} \right] \quad (18)$$

Inserting eqn (7):

$$\frac{\partial^2 x}{\partial \psi \partial T} = \frac{\partial x}{\partial T} \left[1 - \frac{v}{1-x} \frac{\partial x}{\partial \psi} \right] \quad (19)$$

This is a differential equation for

$$\frac{\partial x}{\partial \psi} = f(T) \quad (20)$$

According to (17), that particular solution (20) of eqn (19) must be found which complies with parameter vector x^0 . Then the following actual quantities have to be inserted in (19):

$$\left. \begin{aligned} x(T) &= x(x^0, T) \\ \frac{\partial x}{\partial T} &= \frac{\partial}{\partial T} x(x^0, T) \\ v &= v^0 = x_3^0 \end{aligned} \right\} \quad (21)$$

The differential equation may be solved numerically, using a standard method. According to (17) the desired matrix coefficients are then identical with discrete points of the solution curve.

C_{i2} . Starting with

$$C_{i2} \equiv \left. \frac{\partial x}{\partial E} \right|_{\substack{x=x^0 \\ T=T_1}} \quad (22)$$

one obtains in an analogous manner, again for $v \neq -1$

$$\frac{\partial^2 \alpha}{\partial E \partial T} = - \frac{\partial \alpha}{\partial T} \left[\frac{1}{RT} + \frac{v}{1-\alpha} \frac{\partial \alpha}{\partial E} \right] \quad (23)$$

This is a differential equation for

$$\frac{\partial \alpha}{\partial E} = g(T) \quad (24)$$

leading to the coefficients C_{i2} by numerical solution for the appropriate special conditions (cf. 22).

$$C_{i3} \cdot C_{i3} \equiv \frac{\partial \alpha}{\partial v} \Big|_{\substack{x=x^0 \\ T=T_1}} \quad (25)$$

Considering

$$\begin{aligned} \frac{\partial}{\partial v} [\{1 - \alpha(v)\}^v] &= \frac{\partial}{\partial v} \exp [v \ln \{1 - \alpha(v)\}] \\ &= \exp [v \ln (1 - \alpha)] \left[\ln (1 - \alpha) + \frac{v}{1 - \alpha} \left(- \frac{\partial \alpha}{\partial v} \right) \right] \\ &= (1 - \alpha)^v \left[\ln (1 - \alpha) + \frac{v}{1 - \alpha} \left(- \frac{\partial \alpha}{\partial v} \right) \right] \end{aligned} \quad (26)$$

together with (7) the following differential equation results

$$\frac{\partial^2 \alpha}{\partial T \partial v} = \frac{\partial \alpha}{\partial T} \left[\ln (1 - \alpha) - \frac{v}{1 - \alpha} \frac{\partial \alpha}{\partial v} \right] \quad (27)$$

This is an equation for

$$\frac{\partial \alpha}{\partial v} = h(T) \quad (28)$$

yielding the matrix coefficients C_{i3} .

2.3. Algorithm and program

The method just described was performed in a FORTRAN-program in such a way that after input of the appropriately prepared experimental ("measured") conversion vector and parameters (process parameters, initial assessments of kinetic parameters), an automatic unattended run-off of the program is assured. Program-size: about 30 kbyte. For the numerical integration of the differential equations occurring, the well-known 4-th order method of Runge-Kutta¹⁰ was chosen, using step sizes of 1°C to compute the conversion curves (eqn (7)) and of 2°C for the matrix coefficients (eqns (19), (23), (27)).

The smaller step size for α , $\partial\alpha/\partial T$ became necessary because in the calculation procedure for the matrix coefficients, these quantities are needed at half distance between the abscissa values of two adjacent points.

Systems of normal equations generally show positive definite matrices owing to their special form (16). Therefore, they may be solved by using the Cholesky method. Problems with badly conditioned matrices (break-off of computation-run due to singular matrices of normal equations) only appeared during runs with very extreme initial assessments of parameters. In such cases, the orthogonalization method might be advantageous.

A prerequisite for the intended automatic run of the program is reliable convergence of the iteration procedure within acceptable time. To this end, two measures were taken: first an initial iteration procedure was introduced in order to improve the initial assessments and secondly the step length was limited.

The initial iteration procedure is also performed as non-linear regression, analogous to the proceeding described above, with the modification that only ψ is kept variable while E and v are fixed. The gradient matrix is reduced to a vector and is identical with the first column of the original matrix C .

Even with very erroneous assessments of E , v this initial iteration changes the computed conversion vector in such a manner that the mean value $\alpha = 0.5$ is attained at approximately the same temperature as with the measured conversion curve. This is extremely important as regards convergence.

In comparison with the gradient method⁶, the main advantage of the regression analysis consists in determining not only the direction of the correction vector Δx in parameter space but also its length, thus reducing the number of necessary iteration steps.

On the other hand with increasing step length there is a risk of divergence, since then the basic linear approximation is less and less complied with. For that reason, control of step length with limitation of the tolerable maximum value was inevitable.

Such control was performed for component Δx_2 with critical value x_c , whereby in the case of actual limitation the whole vector Δx was of course shortened.

The tolerable limit x_c is considered as dynamic quantity respecting succeeding iteration steps; its change was made dependent on fulfilling a criterion regarding the mean residue ρ between calculated and measured conversion curves. Explicitly, this criterion demands decreasing residues in sequential iteration steps (this may always be assured with sufficiently small steps) until the actual residue has become smaller than the initially chosen critical value ρ_{cr} . In subsequent steps only the requirement

$$\rho < \rho_{cr}$$

has to be fulfilled.

Generally, the permitted step length x_c is adapted as follows

If the residue criterion is infringed on, x_c is halved.

In the opposite case x_c is doubled, provided Δx has been shortened in the two preceding steps without violation of the residue criterion.

TABLE 1

NUMBER OF ITERATION STEPS FOR DIFFERENT SETS OF INITIALLY ASSESSED KINETIC PARAMETERS

Run	Assessed values of kinetic parameters			Resulting number of iteration steps	
	F (s^{-1})	E ($kcal\ mol^{-1}$)	ν	N_{init}	N_{main}
1	1	30	0	6	4
2	10^{10}	70	0	10	8
3	10^{10}	100	0.5	10	7
4	10^{10}	60	0.5	2	3

3. RESULTS WITH SIMULATED CONVERSION CURVES

3.1. Convergence of the iteration procedure

The behaviour of the iteration procedure towards convergence was tested with a simulated ideal conversion curve, using the following parameter values: $F = 10^{10}\ s^{-1}$; $E = 50\ kcal\ mol^{-1}$; $\nu = 1$; $\Phi = 1^\circ C\ min^{-1}$; $\Delta T_1 = 0.5^\circ C$ for integration of the differential equation; $\Delta T = 2^\circ C$ discretization interval during iteration procedure. The evaluation was performed in the range $0.3 < \alpha \leq 0.9$, i.e., with 13 measuring values and the following critical quantities: $x_c = 10\ kcal\ mol^{-1}$ and $\rho_{cr} = 0.1$. The number of necessary iteration steps depends largely on the initial assessment of the kinetic parameters, cf. Table 1.

Large step numbers appear during runs 2 and 3. With regard to the initial iteration procedure, they may be attributed to the fact that at very unfavourable initial assessments the relative break-off criterion (mean residue less than a fixed critical value) may never be fulfilled and the maximum number of 10 cycles has to be run. In the main iteration, the large number of steps must be traced back to under-shoot of the kinetic parameters in the course of the procedure.

The practically occurring cases are better represented by run 4, where during iteration the parameter values converge predominantly in a uniform way against the

TABLE 2

PROGRESS OF VALUES OF KINETIC PARAMETERS DURING ITERATION PROCEDURE (RUN 4)

Step- No	F ($1/s$)	E ($kcal\ mol^{-1}$)	ν	ρ
0	$4.034 \cdot 10^{10}$	60.000	0.5000	$7.8 \cdot 10^{-2}$
1	$3.908 \cdot 10^{10}$	52.147	1.0021	$7.8 \cdot 10^{-3}$
2	$1.047 \cdot 10^{10}$	50.070	1.0039	$2.1 \cdot 10^{-4}$
3	$1.000 \cdot 10^{10}$	50.000	1.0000	$5.7 \cdot 10^{-4}$

true values (cf. Table 2); therefore only few iteration cycles are required. Additionally this table shows the effect of the initial iteration procedure on the frequency factor, which is raised from the initially assessed value of 10^{10} to $4 \cdot 10^{12} \text{ s}^{-1}$ (associated step-number: 0).

On the available minicomputer system the necessary time per iteration step amounted to: initial iteration, 28 s; main iteration, 50 s, giving a total computing time (without input of data) of 3.5 min for the typical run 4.

Concerning the integration of the differential equations, it should be borne in mind that larger step lengths were used for evaluation than for simulation. Despite this fact, no discrepancies occurred and it must be concluded that even with step lengths of $\Delta T_1 = 1^\circ\text{C}$ resp. 2°C , as applied during evaluation, the relevant discretization errors are negligible.

3.2. Results with simulation curves containing fluctuations

Conversion curves are often determined by use of thermogravimetry (TG). The appropriate weight measurements are always subject to minor statistical fluctuations, caused by disturbances in the furnace, these being particularly strong in flowing atmosphere at reduced pressure. This is manifested in the conversion curves in the form of a superimposed noise component.

The FC-evaluation-method, as an alternative to the NLR-procedure, is known as fairly sensitive to such fluctuations. In order to obtain more insight into the relative properties, a comparison was carried out.

The noise component was simulated by making use of a random generator with normal distribution and a mean of $\mu = 0$. Starting with the above-mentioned ideal conversion curve, several noise-containing curves were produced by addition of noise components of various amplitudes (characterized by the mean deviation σ).

The FC-method is based upon the following equation, obtained from (4) by taking first logarithms, then differences and finally dividing by $\Delta[\ln(1 - \alpha)]$:

$$\underbrace{\frac{\Delta \left[\ln \left(\frac{dx}{dT} \right) \right]}{\Delta A}} = v - \frac{E}{R} \underbrace{\frac{\Delta \left(\frac{1}{T} \right)}{\Delta [\ln(1 - \alpha)]}} \quad (29)$$

After fitting a straight line to the plot ΔA versus ΔB the unknown parameters E , v are supplied by slope and intercept of the line.

The method was implemented so as to conform to the needs of TG-measurements, where $\alpha(T)$ is considered as primary quantity and dx/dT is derived therefrom by numerical differentiation, using local approximation by polynomials of 3rd order. The differences required in eqn (29) are taken between adjacent measuring points, providing no essential deviations from the alternative possibility with a fixed reference point. On the contrary, the arbitrariness always present in the latter case⁴ is removed.

Following the simulation procedure mentioned above, noise-containing

TABLE 3

ERRORS (RMS-VALUES) OF KINETIC PARAMETERS DUE TO DIFFERENT AMOUNTS OF NOISE

σ	<i>Method</i>				
	<i>NLR</i>			<i>FC</i>	
	ΔF_{rel} (%)	ΔE (kcal mol ⁻¹)	$\Delta \nu$	ΔE (kcal mol ⁻¹)	$\Delta \nu$
0	0.0	0.000	0.000	0.020	0.0007
1 · 10 ⁻⁴	2.3	0.035	0.001	5.09	0.10
5 · 10 ⁻⁴	7.8	0.13	0.005	23.8	0.43
1 · 10 ⁻³	15.1	0.25	0.010		
2 · 10 ⁻³	25.0	0.46	0.017		

conversion curves were generated, three at a time with equal standard deviations of noise but individually differing noise components.

The resulting parameter errors evolving from evaluations with the FC- and NLR-method have been assembled in Table 3 as root mean square (RMS)-values of those three curves with equal noise amplitudes. Here, the error associated with the frequency factor has particularly been defined as relative quantity

$$\Delta F_{rel} = \frac{|\Delta F|}{F} \quad (30)$$

Obviously, by the NLR-method as compared with the FC-method an enormously diminished sensitivity to measuring fluctuations has been achieved.

As regards the considerable error of the FC-method, it should not be forgotten that a modified FC-procedure aimed at evaluating DTA/DSC-measurements would show smaller errors at equal noise level because there dx/dT results directly from measurements without the need to resort to numerical differentiation.

4. MEASUREMENTS AND RESULTS

Measurements of the decomposition of CaCO₃ were carried out on a Mettler Thermoanalyzer TA making use of the alumina furnace and a standard alumina crucible (Ø8, height 11 mm). Synthetic powder of CaCO₃ (Merck, p.a.) was used as sample substance, to which after mortaring no further processing was applied.

To enable the sample temperature to rise linearly in time (constant heating rate), the standard temperature control equipment contains, apart from the linearizing electronics, direct contact between temperature sensor and crucible. In this way, temperature deviations caused by the reaction heat are best diminished.

The stream of inert gas was guided from the balance room through the furnace to the pump. An additional throttle valve installed between furnace and pump enabled a separate regulation of pressure and flow-rate. The data logging was done

on paper tape, using the Mettler CT-system for transfer of digital data. Weight data were registered at constant time intervals, being equivalent, due to the time-independent heating rate, to constant-temperature increments.

In this way, from each measuring run, a sequence of weight data (measuring vector) was produced which had to be coordinated with a vector of equidistant temperature values. Every determination of a conversion curve necessitated two measuring runs: one for the proper dissociation reaction and one for the baseline.

Proceeding from two such runs, it is possible to compute the conversion curve as follows. An approximate course of mass diminution is obtained according to

$$\Delta m^*(T) = \frac{1}{g} [G^R(T_0) - G^R(T) - \{G^B(T_0) - G^B(T)\}] \quad (31)$$

where G^R = measured weight data of reaction run; G^B = measured weight data of baseline; T_0 = initial temperature of measurements; g = acceleration of gravity; Δm^* = approximate mass diminution.

As the disturbing forces on the balance arising from the stream of gas, buoyancy of the sample holder and thermomolecular flow occurring at intermediate pressures¹¹ may reasonably be assumed as equal whether a sample is present or not, these forces are eliminated in the above manner.

After an additional correction allowing for the buoyancy of the sample, the true course of mass diminution $\Delta m(T)$ is computed, from which the desired conversion curve is obtained according to

$$\alpha(T) = \frac{\Delta m(T)}{\Delta m_{\text{tot}}} \quad (32)$$

The conversion vector directly yielded the temperature of half conversion, defined by

$$T_{\frac{1}{2}} = T(\alpha = 0.5) \quad (33)$$

Above all, however, it served as vector of input data to the evaluation program performing NLR, where the kinetic parameters were computed relative to desired values for conversion range and temperature increment. Generally used values:

range: $0.3 < \alpha \leq 0.9$

T -interval: $\Delta T = 3$ resp. 4°C for $\Phi = 0.5$ resp. 2°C min^{-1}

In this way, the evaluation took place in all cases with 12 to 20 data points.

Under most of the different conditions, three measuring runs were performed respectively. The means of the resulting parameters E , ν , $T_{\frac{1}{2}}$ are listed in Table 4, together with the related standard deviations, defined by

$$\Delta y_i = \sqrt{\frac{\sum_{i=1}^N (y_i - \bar{y})^2}{N - 1}} \quad (34)$$

TABLE 4

RESULTS OBTAINED BY EVALUATION OF MEASUREMENTS WITH NON-LINEAR REGRESSION PROCEDURE

<i>Mode</i>	<i>N</i>	<i>Afm</i>	<i>P</i> (Torr)	<i>Q*</i> (ml/min ⁻¹)	<i>φ</i> (°C/min ⁻¹)	<i>m₀</i> (mg)	<i>T₁</i> (°C)	<i>F_M</i> (s ⁻¹)	<i>E</i> (kcal mol ⁻¹)	<i>ν</i>	<i>ρ</i> (10 ⁻³)
I	3	N ₂	720	30	2	10	674.5 ± 1.8	4.9 · 10 ⁹	56.0 ± 2.0	0.21 ± 0.02	0.8
II	3	N ₂	720	30	0.5	10	628.2 ± 0.3	2.6 · 10 ⁹	54.5 ± 1.1	0.17 ± 0.01	1.0
III	3	He	720	30	0.5	10	609.1 ± 0.3	2.0 · 10 ¹⁰	56.7 ± 1.0	0.25 ± 0.01	0.7
IV	1	He	720	30	0.5	5	582.8	4.8 · 10 ⁹	52.6	0.41	1.6
V	1	He	50	0	0.5	10	567.5	1.3 · 10 ¹⁰	60.7	0.39	1.0
VI	1	He	5	0	0.5	10	550.3	1.4 · 10 ¹⁰	59.5	0.49	0.6
VII	3	He	1	1	0.5	10	529.3 ± 1.4	1.5 · 10 ¹⁰	72.2 ± 0.9	0.77 ± 0.03	0.8
VIII	1	He	1	1	0.5	5	521.9	2.6 · 10 ¹⁰	83.1	0.88	3.3
IX	3	He	1	6	0.5	5	485.3 ± 3.6	2.4 · 10 ¹⁰	68.6 ± 6.7	1.53 ± 0.09	6.0
X	3	Vak.	10 ⁻⁸	0	0.5	5	494.2 ± 4.2	5.1 · 10 ⁹	36.7 ± 2.6	0.79 ± 0.11	2.6

The specified frequency factor represents a multiplicatively averaged-out value

$$F_M = \left[\prod_{i=1}^N F_i \right]^{1/N} \quad (35)$$

corresponding to the arithmetic mean of the frequency variable ψ .

Noticeable from the viewpoint of measuring techniques appears the bad reproducibility of T_x and kinetic parameters respecting measurements IX and X.

The measurements of case IX are carried out at 1 Torr and relatively high rates of gas-flow. Extremely strong disturbing forces result, as seen in the baselines. They cause a larger noise level of 5 μg , increased by factor 4, compared to measurements performed at normal pressure. For 5-mg samples with a total mass diminution of 2.2 mg this means a noise component

$$\sigma = 2.3 \cdot 10^{-3}$$

relative to the entire conversion.

According to the results of Table 3, this is too high a value to employ the FC-method, while no problems exist as regards the NLR-procedure. However, a considerably larger statistical parameter-error is observed in practice than would be expected from noise alone. The additional disturbance apart from noise must be due to irregularities in the gas flow leading to relatively stronger statistical errors at higher flow-rates.

In the case of vacuum measurements X, the reason for the increased error must be traced to the lower heat conductivity within the sample under those conditions. Minor differences in packing density may then cause slight variations in the conversion curves.

5. DISCUSSION

The main objective has been attained. A new method has been developed on the basis of non-linear regression, allowing us to determine kinetic parameters from measurements with generally good reproducibility.

However, from the considerable dependence on measuring conditions, we may conclude that kinetics are determined by several different processes.

The reaction step



is considered as chemically rate-controlling process; where CaO^* represents an activated state which is only reached by use of the appropriate activation energy. A chemical substance is of course most specifically characterized by a process of such nature.

As concurrent processes, the diffusion of heat and/or CO_2 -gas have to be taken into account. Due to non-ideal heat-diffusivity in the sample, the endothermal reaction heat induces an inhomogeneous temperature distribution and therefore subcooling within the sample, thus reducing the actual rate of reaction, whereas the non-vanishing partial pressure CO_2 gives rise to partial reverse reaction. These two

competing processes may even dominate¹². In such cases, it may be expected that, apart from depending on the measuring conditions, the related kinetic parameters characterize predominantly the texture (grain size and compactness of the sample), a fact which may be of importance with respect to corresponding applications.

Hence, the question arises of how to interpret the results and which of the parameters correspond best to the true values of the chemically controlled kinetics.

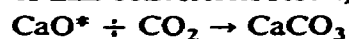
As both diffusion processes, contrary to the activation step of the chemical reaction, may be largely influenced by variations of the gas flow conditions, lower values of $T_{\frac{1}{2}}$ which may be attained under favourable conditions indicate an augmented chemical nature of the kinetics control. This statement holds good of course only for fixed heating rate, since with otherwise identical processes, larger heating rates are followed by larger values of $T_{\frac{1}{2}}$.

Considering first only vacuum measurements, in comparison with all the other measurements they are characterized by:

least hindrance of reaction with regard to CO_2 partial pressure

greatest hindrance in respect of heat transport (as in a high vacuum this is considerably lower than in flowing Helium gas as used in the other measurements)

Since with nearly all measurements (exception: IX), higher values of temperature of half-conversion result, we suppose that there the reverse reaction



induced by the partial pressure of CO_2 is rate-controlling. In order to understand the reaction, a more detailed investigation of this phenomenon is therefore indicated.

5.1. Influence of the partial pressure of CO_2 on the dissociation kinetics of CaCO_3

Dispensing with one of the ideal assumptions by also admitting the presence of partial pressure of carbon dioxide, the basic eqn (4) characterizing the kinetics must be modified. Assuming the experimentally verified linear dependence of the reaction rate on partial pressure of CO_2 ^{13, 14} one obtains the following new equation

$$\frac{dx}{dT} = \frac{F}{\Phi} e^{-E/RT} (1-x)^y [1 - \gamma(T)] \quad (36)$$

with

$$\gamma(T) = \frac{P_P(T)}{P_D(T)} \quad (37)$$

where γ = correction quantity; P_P = partial pressure of CO_2 ; P_D = dissociation pressure of CaCO_3 .

Within limited temperature ranges the temperature dependence of the dissociation pressure may be described according to the general approximate law

$$P_D(T) = P_D^\infty e^{-E_D/RT} \quad (38)$$

where E_D = dissociation enthalpy of CaCO_3 ; P_D^∞ = proportionality constant,

representing in this approximation the dissociation pressure at temperature $T \rightarrow \infty$.

With the additional assumption of immediate mixing of decomposition and flow-gas, there results within the whole gas phase a homogeneous CO_2 -partial-pressure, which may be calculated as follows:

$$P_F = P_F \frac{\dot{n}_D}{\dot{n}_F} \quad (39)$$

$$\dot{n}_D = \frac{m_0}{m_M} \frac{dx}{dt} = \frac{m_0}{m_M} \phi \frac{dx}{dT} \quad (40)$$

$$\dot{n}_F = \frac{Q_F}{V_M} \quad (41)$$

therefore

$$P_F(T) = P_F \frac{V_M}{Q_F} \frac{m_0}{m_M} \phi \frac{dx}{dT} \quad (42)$$

with \dot{n}_D = molar flow of decomposition-gas (mol s^{-1}); \dot{n}_F = molar flow of flow gas (inert gas); P_F = pressure of flow gas; m_0 = initial mass of sample; m_M = molar mass of sample; V_M = molar volume of flow gas at normal conditions (P_0, T_0); Q_F = volume flow of flow gas, converted to normal conditions.

inserting (42) in (37) yields

$$\gamma(T) = \frac{z}{P_D(T)} \frac{dx}{dT} \quad (43)$$

with the temperature-independent constant

$$z = \frac{V_M}{Q_F} \frac{m_0}{m_M} \phi P_F \quad (44)$$

Insertion of (43) in (36):

$$\frac{dx}{dT} = \left(\frac{dx}{dT} \right)_{id} \left[1 - \frac{z}{P_D(T)} \frac{dx}{dT} \right] \quad (45)$$

Here $(dx/dT)_{id}$ represents the formal expression for the ideal reaction rate, given by eqn (4). Solving dx/dT , we obtain together with (38)

$$\frac{dx}{dT} = \frac{\left(\frac{dx}{dT} \right)_{id}}{1 + \frac{z}{P_D^0} e^{E_D/RT} \left(\frac{dx}{dT} \right)_{id}} = \frac{\frac{F}{\phi} e^{-E/RT} (1 - \alpha)^r}{1 + \frac{zF}{P_D^0 \phi} e^{(E_D - E)/RT} (1 - \alpha)^r} \quad (46)$$

This is the differential equation for the real conversion curve $\alpha(T)$, where the partial pressure of the decomposition gas has additionally been allowed for. Numerical integration may again be performed by making use of the Runge-Kutta method.

TABLE 5

INFLUENCE OF KINETIC PARAMETERS AND OF GAS-FLOW CONDITIONS ON NON-IDEAL BEHAVIOUR OF DISSOCIATION PROCESS (DUE TO NON-VANISHING PARTIAL PRESSURE OF CO₂); SIMULATED AND EXPERIMENTAL CONVERSION CURVES

No.	Mode	m_0 (mg)	ϕ (°Cmin ⁻¹)	F (s ⁻¹)	E (kcalmol ⁻¹)	ν	P_F (Torr)	Q_F (nmlmin ⁻¹)	α_m	γ_m (%)	$T_{\frac{1}{2}}^r$ (°C)	$T_{\frac{1}{2}}^i$ (°C)	$\Delta T_{\frac{1}{2}}$ (°C)
1		5	2	10 ¹⁰	50	1	720	30	0.16	57.4	585.5	564.1	21.4
2		5	0.5	10 ¹⁰	50	1	720	30	0.17	50.5	545.3	529.3	16.0
3		10	0.5	10 ¹⁰	50	1	720	30	0.18	68.8	556.7	529.3	27.4
4		5	0.5	10 ¹⁶	70	1	720	30	0.37	74.6	534.8	513.0	21.8
5		5	2	10 ¹⁰	50	1	1	5	0.17	1.0	564.3	564.1	0.2
6		5	0.5	10 ¹⁰	50	1	1	5	0.17	0.8	529.4	529.3	0.1
7		10	0.5	10 ¹⁰	50	1	1	5	0.17	1.5	529.6	529.3	0.3
8		5	0.5	10 ¹⁶	70	1	1	5	0.35	1.5	513.2	513.0	0.2
9	I	10	2	4.9 · 10 ⁹	56.0	0.21	720	30	0.59	11.4	679.7	674.6	5.1
10	III	10	0.5	2.0 · 10 ¹⁰	56.7	0.25	720	30	0.55	15.5	612.3	608.8	3.5
11	IX	5	0.5	2.4 · 10 ¹⁶	68.6	1.53	1	6	0.23	3.1	486.9	486.4	0.5
12		10	0.5	2.4 · 10 ¹⁶	68.6	1.53	1	6	0.25	6.1	487.3	486.4	0.9
13		5	0.5	2.4 · 10 ¹⁶	68.6	1.53	720	30	0.30	91.8	526.6	486.4	40.2
14		50	0.5	2.4 · 10 ¹⁶	68.6	1.53	720	30	0.30	99.8	596.3	486.4	109.9

The progress of the correction quantity with temperature may then be obtained by considering eqns (43) and (44)

$$\gamma(T) = \frac{V_M}{Q_F} \frac{m_0}{m_M} \Phi \frac{P_F}{P_D(T)} \frac{dz}{dT} \quad (47)$$

From measurements of Hill and Winter¹⁵ concerning the decomposition pressure of CaCO_3 , the following numerical values are obtained: $P_D^\circ = 2.525 \cdot 10^{10}$ Torr and $E_D = 40.221 \text{ kcal mol}^{-1}$.

The correction quantity $\gamma(T)$ has been calculated for different parameter triples, these corresponding to results from measurements as well as to further typical parameter combinations.

In Table 5 the resulting values of the following quantities have been listed:

γ_m = maximum value of $\gamma(T)$

$\alpha_m \equiv \alpha|_{\gamma=\gamma_m}$

$T_{\frac{1}{2}}^i$ = temperature of half conversion of an ideal conversion curve

$T_{\frac{1}{2}}^r$ = ditto for a real conversion curve

$\Delta T_{\frac{1}{2}} \equiv T_{\frac{1}{2}}^r - T_{\frac{1}{2}}^i$

Generally, large γ_m -values occur with respect to 720 Torr-runs, indicating the presence of relatively high partial pressures of CO_2 . At the same time, simulation runs 1 to 8 clearly show that, with fixed kinetic parameters, every reduction of pressure is accompanied by a considerable decrease in γ_m and therefore in $T_{\frac{1}{2}}$; this holds without considering m_0 , Φ , E . Therefore, by performing the measurements at low pressure, the influence of the reverse reaction may drastically be reduced.

A further indication that low pressure conditions are more favourable is seen from the dependence of $T_{\frac{1}{2}}$ on sample mass m_0 . With the 1 Torr-measurements VII, VIII, although performed at relatively low gas flow, a much lower dependence results in comparison with the 720 Torr-measurements III, IV (cf. Table 4).

The simulations performed are all based on the assumption of immediate mixing of gases effecting homogeneous CO_2 -gas-concentration in the whole gas phase. Deviations from this concept may be described by a factor δ_{eff} representing the ratio between the real concentration of carbon dioxide near reacting sample grains and the ideal homogeneous concentration.

This factor causes an increase of the effective partial pressure P_p ; thus one obtains:

$$\alpha_{\text{eff}} = \delta_{\text{eff}} \alpha \quad (48)$$

with the corresponding effects on $\gamma(T)$ and $\alpha(T)$.

In the simulation procedure, instead of introducing the factor δ_{eff} explicitly, the same effect may also be obtained by an equivalent increase of the effective sample mass

$$m_0 \rightarrow \delta_{\text{eff}} m_0$$

as may be concluded from equations (48) and (44).

From the above-mentioned facts, ideal mixing of gases (and therefore $\delta_{eff} = 1$) under the best measuring conditions may be assumed with good reason.

Numerical values of δ_{eff} for the 720 Torr-conditions may then be obtained by comparing the differences $\overline{\Delta T_{\frac{1}{2}}}$, defined by

$$\overline{\Delta T_{\frac{1}{2}}} \equiv T_{\frac{1}{2}}(P_F = 720 \text{ Torr}) - T_{\frac{1}{2}}(P_F = 1 \text{ Torr}) \quad (49)$$

both for measurements IV, IX (Table 4) on the one hand and for simulations 11, 13, 14 (Table 5) on the other.

From the measurements, a difference of $\overline{\Delta T_{\frac{1}{2}}} = 97.5^\circ\text{C}$ results. This same amount may be obtained by interpolation from the simulation runs only by using about the 8-fold sample mass in the 720-Torr run. Therefore, a factor $\delta_{eff} \approx 8$ has to be considered under such conditions.

The rather large differences in the γ_m -values occurring within simulation curves corresponding to the higher pressure conditions (720 Torr), viz., runs 9, 10 \leftrightarrow 13 (Table 5) appear obscure at first sight. While in the former two runs, kinetic data are used relating to measurements carried out at this same pressure, in the latter run 13 we employ kinetic parameters experimentally determined at 1 Torr and extrapolate to the higher pressure conditions.

Considering first that processes most adequately described by eqn (36) were evaluated with (4) after measurement, and that secondly, according to the results of simulation-runs 1 to 8, the discrepancies between these two model equations must increase with pressure (while of course no differences exist at infinitesimal pressure), one is led to suppose that the above-mentioned obscure findings may be directly connected to the pressure-dependent model incompatibilities, these being large in case of runs 9 and 10 measured at higher pressure, while negligible for run 13 (low-pressure conditions).

If so, we would have to conclude that according to runs 9 and 10, measurements performed at higher pressures after evaluation with (4) yield considerably too low γ_m -values and correspondingly deviating kinetic parameters.

Therefore, under conditions of higher flow-gas pressures, the supposed control of kinetics by the reverse reaction due to the presence of carbon dioxide in the gas phase has been confirmed: CO_2 -partial-pressures are almost equal to the equilibrium dissociation pressure and therefore γ_m -values approaching unity occur. The actual, effective values of partial pressure, represented by the related correction quantities γ_m^{eff} even exceed the γ_m -values reported in Table 5, due to the fact that $\delta_{eff} > 1$ under such conditions.

The situation appears quite different for kinetic measurements conducted under low-pressure conditions. The reduced influence of CO_2 -diffusion is seen from the low value of 0.03 occurring for the correction quantity γ_m , as concerns the best measurements IX, represented by simulation run 11. A further reduction of γ_m might be possible by using a smaller sample mass.

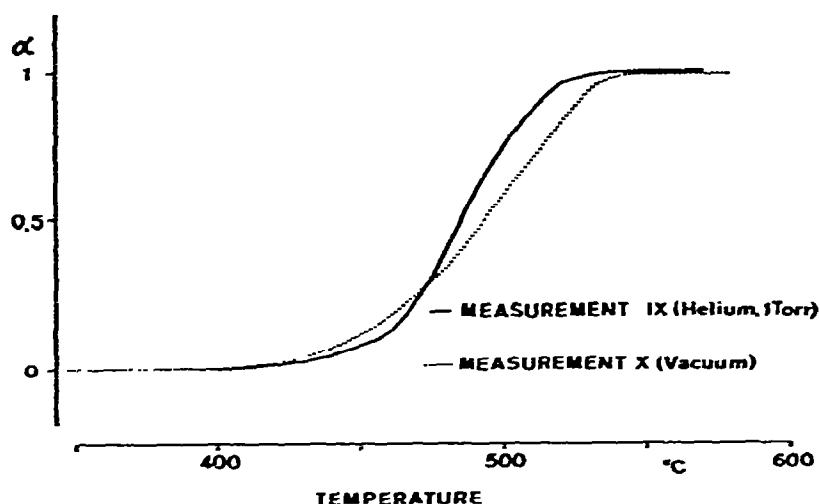


Fig. 2. Conversion curves.

5.3. Influence of thermal conductivity on the decomposition kinetics

At first sight, decrease in temperature of half-conversion by changing the flow gas from nitrogen to helium (measurements II, III under otherwise equal conditions) appears remarkable. At least partially, this has to be ascribed to a better heat exchange within the sample owing to the better heat conduction of helium-gas. Besides, changed flowing conditions may occur influencing the exchange of heat and/or CO_2 between sample and convective flow gas.

Heat transfer may even appear as rate-controlling, as is obvious from measurements X in high vacuum, mainly by comparing with the optimal measurements IX in 1 Torr helium (Figure 2). Though in high vacuum, the decomposition already starts at lower temperatures, clearly caused by the vanishing partial pressure of CO_2 , the conversion curve shows a considerably lower slope, so that half-conversion is attained at an even higher temperature. Moreover, completely changed values of activation energy result. These effects must be attributed to the lower heat exchange in high vacuum.

5.4. Conclusions

In order to determine the kinetic parameters for the decomposition of CaCO_3 , the conditions of measurements IX turned out to be most favourable, i.e., low sample mass, low heating rate, helium gas flow at a pressure of about 1 Torr and with high flow-rate. In this way, the systematic errors caused by the partial pressure of CO_2 (reverse reaction) may be greatly reduced. Moreover, at a pressure of 1 Torr the heat exchange within and to the sample is still adequate, since in the viscous pressure range, heat conductivity of ideal gases is independent of pressure, while it decreases below 1 Torr.

On the other hand, under these conditions the largest statistical errors appear.

Therefore, the highest requirements have to be met with regard to measuring and evaluation.

In this case, the high measuring fluctuations render it impossible to evaluate according to the Freeman-Carroll procedure, whereas the described new method using non-linear regression may be applied without any difficulty.

Furthermore, one becomes aware that beyond noise additional disturbances occur affecting reproducibility. Assuming that the resulting mean residues are exclusively due to noise, by extrapolation of the results given in Table 3 the following evaluation errors ensue: $\Delta E = 1.5 \text{ kcal mol}^{-1}$ and $\Delta v = 0.06$. The considerably higher statistical error ΔE resulting from measurement IX must therefore be ascribed to experimental shortcomings.

In future measurements, attention has above all to be paid to the elimination of instabilities in the gas flow and to the use of samples with defined grain size.

REFERENCES

- 1 J. Zsakó and H. E. Arz, *J. Therm. Anal.*, 6 (1974) 651.
- 2 P. K. Gallagher and D. W. Johnson, Jr., *Thermochim. Acta*, 6 (1973) 67.
- 3 J. H. Sharp and S. A. Wentworth, *Anal. Chem.*, 41 (1969) 2060.
- 4 J. Šesták, V. Šatava and W. W. Wendlandt, *Thermochim. Acta*, 7 (1973) 464.
- 5 E. S. Freeman and B. Carroll, *J. Phys. Chem.*, 62 (1958) 394.
- 6 H. H. Rosenbrock and C. Storey, *Computational Techniques for Chemical Engineers*, Pergamon Press, New York, 1966, ch. 4.
- 7 A. C. Norris, M. I. Pope and M. Selwood, *J. Therm. Anal.*, 9 (1976) 425.
- 8 D. W. Marquardt, *J. Soc. Ind. Appl. Math.*, 11 (1963) 431.
- 9 H. R. Schwarz, H. Rutishauser and E. Stiefel, *Numerik symmetrischer Matrizen*, Teubner, Stuttgart, 1968, p. 82.
- 10 P. Henrici, *Discrete Variable Methods in Ordinary Differential Equations*, Wiley, New York, 1962, p. 68.
- 11 C. H. Massen and J. A. Poulis, in S. P. Wolsky and E. J. Zdanuk (Eds.), *Ultra Micro Weight Determination in Controlled Environments*, Interscience, New York, 1969, p. 112.
- 12 A. W. D. Hills, *Chem. Eng. Sci.*, 23 (1968) 297.
- 13 T. R. Ingraham and P. Marier, *Can. J. Chem. Eng.*, 41 (1963) 170.
- 14 J. Zawadzki and S. Bretsznajder, *Trans. Faraday Soc.*, 34 (1938) 951.
- 15 K. J. Hill and F. R. S. Winter, *J. Phys. Chem.*, 60 (1956) 1361.